ACS OMEGA

Open Access

This article is licensed under CC-BY-NC-ND 4.0

http://pubs.acs.org/journal/acsodf

Article

Investigation of Host–Guest Inclusion Complex of Mephenesin with α-Cyclodextrin for Innovative Application in Biological System

Subhajit Debnath, Biswajit Ghosh, Modhusudan Mondal, Niloy Roy, Kangkan Mallick, Joydeb Maji, Sudip Sahana, Anuradha Sinha, Sangita Dey, Anoop Kumar, and Mahendra Nath Roy*

Cite This: ACS Omega 2024, 9, 36066–36075

Read Online

ACCESS | Metrics & More | Article Recommendations | Supporting Information

ABSTRACT: The goal of this study was to use coevaporation to look into how polyether compounds like mephenesin (MEP) can be encapsulated into the host molecule α-cyclodextrin's nanohydrophobic cage. Fourier transform infrared spectroscopy (FT-IR) investigations, powder X-ray diffraction (PXRD), and ^{1}H NMR were among the spectroscopic techniques used to describe the inclusion complex. Additionally, Job's plot has been utilized to illustrate how MEP is encapsulated with α-cyclodextrin (α-CD) at a 1:1 molar ratio. The thermal stability of MEP increased after encapsulation according to thermogravimetric analysis (TGA) and differential thermal analysis (DTA) experiments. Mephenesin fits into the cavity of α-cyclodextrin in a 1:1 ratio, as observed by molecular docking for the inclusion complex to find the most appropriate orientation. This observation is further supported by the Job plot. Furthermore, a comparison was carried out based on a cell viability study between the medication and its inclusion complex.

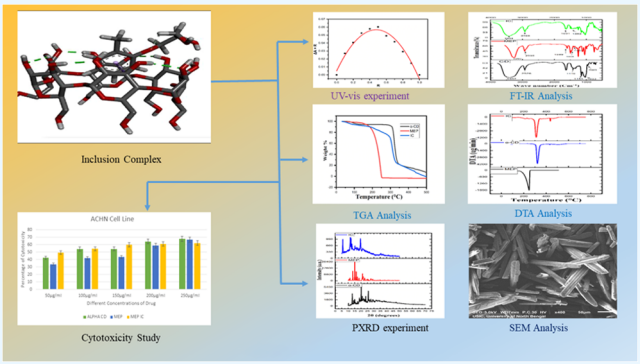

1. INTRODUCTION

Propylene glycol (PG), a polyether compound, is typically utilized as a passive ingredient in injectable and oral pharmaceutical formulations for medications that are either water-insoluble or weakly water-soluble drugs.[1,2] Nevertheless, its derivatives such as the muscle relaxant mephenesin (MEP) and the boron chodilator diprophylline are extremely physiologically active substances made of glycolyl and glyceryl side chains.[3,4] Troxerutin is a venotropic medication that is typically used to treat chronic venous insufficiency (CVI), improve capillary function, and relieve pain. Other venotropic medications include etofenamate and glafenin, which are also anti-inflammatory.[5]

Mephenesin selectively inhibits nerve impulses at particular neurons in the spinal cord, brainstem, and subcortical parts of the brain. It is currently used as a medicine to relax skeletal muscles.[6,7] Early studies indicated that it increases glycine levels, and later research suggested that it could act as an antagonist of excitatory amino acids, possibly explaining its muscle relaxant properties.[8] However, mephenesin also has drawbacks, including its short-lasting effect due to rapid metabolism and a hemolytic side effect causing red blood cell destruction.[9]

Diazepam, mephenesin, and barbiturates are among the helpful sedatives and muscle relaxants that can be used to treat strychnine toxicity. Mephenesin, also known by the name 3-(2-methylphenoxy)propane-1,2-diol, is one of the most significant medications in the glycerol ether family. It is also referred to as a blockbuster medication known as centrally acting skeletal muscle relaxants.[10,11] It dissolves in ethyl alcohol and propylene glycol and is a crystalline solid with no color or odor. MEP specifically acts on spinal interneurons, causing polysynaptic reflex contractions to be inhibited, while monosynaptic knee-jerk reflexes remain unaltered. Pharmacological studies have demonstrated that mephenesin has anticonvulsant and muscle-paralyzing effects. It also exhibits local anesthetic action in vitro but not so much in vivo.[12,13]

Because of their distinctive truncated cone structure, cyclodextrins (CDs) are the most interesting host molecules in the supramolecular field. They may form stable complexes, or ICs, with a variety of guest molecules.[14] The cyclic oligosaccharides known as cyclodextrins (α, β, and γ) consist of six to eight glucopyranose units linked together by α-1,4-linkages. These oligosaccharides have hydrophobic cavities with varying sizes and radii that can accommodate multiple molecules through noncovalent interactions, such as dipolar interaction, electrostatic bonding, and hydrogen bonding. The

Received: October 30, 2023
Revised: July 7, 2024
Accepted: August 8, 2024
Published: August 15, 2024

© 2024 The Authors. Published by American Chemical Society

Scheme 1. Two-Dimensional Structures of MEP and α-CD

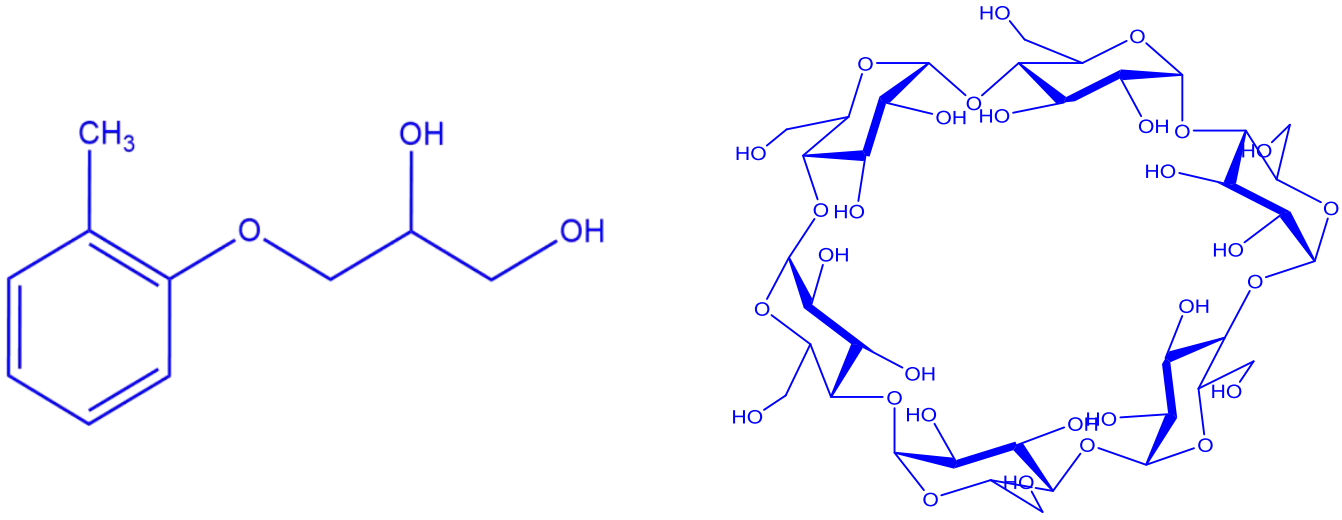

inner area of the CDs allows for the incorporation of hydrophobic surfaces of different guests or segment(s) of any guest molecules into the cavity of suitable and stable geometrical-sized CDs.[15−18]

The establishment of an inclusion complex can progress the solubility, thermal stability, bioavailability of the drug molecule, and also decrease the side effects through the formation of an inclusion complex.[19] The widely used host α-cyclodextrin is often preferred in inclusion complex formation due to its unique structural characteristics. Its smaller cavity size compared to other cyclodextrins, such as β and γ, allows for better accommodation of guest molecules. This can result in increased stability and improved solubility of the inclusion complex, making α-cyclodextrin a favorable choice for certain applications.[20] However, the selection of cyclodextrin depends on the specific properties and requirements of the guest molecule and the desired outcome of IC formation. They have garnered significant attention for their proficiency in forming inclusion complexes with hydrophobic guest molecules, making them useful in various industries, including pharmaceuticals, textiles, food, and more.[21]

In this study, the researchers encapsulated MEP within the nanocavity of α-CD and investigated the complex using various analytical techniques such as UV−visible, IR spectroscopy, powder X-ray diffraction, ^{1}H NMR, thermogravimetric analysis (TGA), molecular modeling, and scanning electron microscopy (SEM). A Job plot suggested a 1:1 stoichiometry for the complex, and UV−visible studies provided insight into the thermodynamic parameters and association constants of the inclusion process. Studies on the survivability of human normal kidney cells in vitro revealed that the inclusion complex was less harmful to the cells than the medication in its pure form. This suggests that the inclusion process may have contributed to the reduction in the toxicity (Scheme 1).

2. EXPERIMENTAL SECTION

2.1. Materials. For this research work, TCI Chemicals India Pvt. Ltd. provided the drug MEP (MW = 182.22 g/mol) with purity >98.0%, and SIGMA-Aldrich India provided the host molecule α-CD (MW = 972.84 g/mol) with purity ≥97%. Water that had been twice distilled was used for all of the trials. The National Centre for Cell Science (NCCS), located in Pune, India, provided the human kidney adenocarcinoma (ACHN) cell line. Cell culture plasticware, penicillin, streptomycin, fetal calf serum (FCS), sodium azide, sodium bicarbonate, phosphate buffer saline, isopropanol, MEM media, and 3-(4,5-dimethylthiazol-2-yl)-2,5-diphenyl tetrazolium bromide (MTT) were purchased from Hi Media, India.

2.2. Instruments. The Agilent 8453 UV−vis spectrophotometer was used to analyze the materials and determine their UV−visible spectra. A Bruker AVANCE DRX 400 NMR spectrometer operating at 400 MHz was utilized to acquire the ^{1}H NMR spectra at 298.15 K. Using a PerkinElmer FT-IR spectrometer having a 400−4000 cm^{-1} range and a 4 cm^{-1} resolution, the FT-IR spectra of samples as KBr pellets were recorded. Powder X-ray diffraction (XRD) measurements were collected using a German-made Bruker D8 Advance instrument. The samples' surface morphology was captured by the use of a JSM-6360 scanning electron microscope (SEM) to capture photographs. A PerkinElmer Diamond TG/DTA analyzer was used to examine the samples' thermal analysis (TGA, DTA) in a clean N_2 gas environment (1.5 atm) between 25 and 500 °C.

2.3. Sample Preparation. A very well-known technique, i.e., coprecipitation, was used to synthesize the inclusion complex. First, 40 mL of distilled water was used to combine 0.138 g of α-CD and 0.26 g of MEP. After that, the reaction mixture was stirred for 48 h at 58 °C. The final product was filtered, rinsed three times with an ethanol−water mixture, and allowed to dry for a full day. Ultimately, the final product was gathered and preserved for storage in a vacuum desiccator.

2.4. Preparation of Three-Dimensional (3D)-Structures of MEP and α-CD. The PubChem website (http://pubchem.ncbi.nlm.nih.gov) provided the three-dimensional structures of MEP. α-CD was extracted from a complex belonging to Cambridge Crystal Data Centre (CCDC), with deposit number CCDC ID: 125105.[22] Before the computational studies were conducted, using Gaussian 09 software, the DFT-B3LYP approach was used to optimize each structure. To both α-CD and MEP, missing hydrogen atoms and atomic charges were added.[23]

2.5. Molecular Docking Evaluation. A computational method called "molecular docking" aids in the prediction of a guest's primary way of interaction with a host.[24] For the host−guest system developed in PyRx, a well-established docking technique was used.[25] Prior to docking, PyRx docking software

https://doi.org/10.1021/acsomega.3c08185
ACS Omega 2024, 9, 36066−36075

was used to produce atomic coordinates from PDB files of MEP and α-CD that had been translated into the PDBQT format. The dimensions of the grid box were set to size x = 25, size y = 25, and size z = 25 for each of the three coordinates. The center values were set to center_x = 69.657, center_y = 88.1966, and center_z = 56.0492. To allow for the easy movement of the ligand MEP within the search space, the size of the grid box enclosing the binding pocket of the α-CD receptor was selected. The lowest-energy docked conformer was selected based on the docking score, and Discovery Studio Visualizer, v21.1.0.20298, BIOVIA, was used for the visualization.[26]

2.6. MTT Assay. Human renal adenocarcinoma (ACHN) cells were maintained in minimum essential medium Eagle's (MEM) media containing 10% fetal calf serum (FCS), 100 units/mL of penicillin, 100 μg/mL of streptomycin, and 2.2 g/L of sodium bicarbonate in 100 mm of petriplate at 37 °C, 5% CO_2 incubator for further experiments.[27] The ACHN cells were seeded at a density of 5 × 10^3 cells each well into a 96-well microtiter plate and incubated in a CO_2 incubator for 24 h at 37 °C and 98% humidity. The next day, drugs (α-CD, MEP, MEP-IC) were added at various concentrations (50, 100, 150, 200, 250 μg/mL) dissolved in distilled water in triplicate and placed in for the same condition for 24 h. The next day, the media was discarded and after that, 10 μL of MTT dye solution (stock solution 5 mg/mL freshly prepared in 1× PBS) was added to each well and placed for 3 h of incubation. Following an incubation period of 3 h, the purple formazan crystals were dissolved by adding 50 μL of isopropanol to each well. Then, the plate was gently shaken for 5 min and the absorbance was measured at 620 nm on a Spectro Star Nano Spectrophotometer. The percentage of cytotoxicity was calculated as the percentage of cytotoxicity (%) = $\{(Y - X)/Y \times 100\}$, where X is the mean OD of drug-treated cells and Y is the mean OD of blank cells.[28,29]

3. RESULTS AND DISCUSSION

3.1. NMR Study. Using ^{1}H NMR, one may verify whether an IC is formed between the host and guest molecules.[30] The drug molecule was inserted into the hydrophobic cavity of the host α-CD, causing the protons of MEP and α-CD molecules to shift in their chemical shifts.[31,32] The protons H1, H2, and H4 are positioned on the outside of the α-CD molecule, but the H3 and H5 protons of the α-CD are inside the cavity and near the wider and narrower sides, respectively.[33,34] Table 1 lists the chemical shift values for the MEP, α-CD, and their IC and shows that the NMR signals of the H3 and H5 protons from α-CD have moved upfield, indicating that IC with the MEP molecule has formed, signifying that the drug MEP goes into the hydrophobic cage from the wider edge.[35] As Table 1 shows, it is also well-documented that the signals associated with the H1, H2, H4, and H6 protons of α-CD accompanied by or without MEP are almost the same since they are positioned on the external surface. Significant downfield shifts in the aromatic protons of MEP suggest that the molecule is encapsulated inside the cavity of the α-CD ring (Figure 1).[36,37] These results validate the new IC's development.

3.2. FT-IR Spectroscopy. The IC development phenomena are resolved using FT-IR spectroscopy by accounting for the peak shape position and peak intensity.[38,39] Figure 2 displays the FT-IR spectra of the pure α-CD, MEP, and solid IC. The guest molecule MEP revealed absorption bands at around 3260 cm^{-1} for the −OH stretching vibration; this could be because the guest molecule has two adjacent −OH groups that are likely to form a H-bond. In the $-CH_3$ group, the −CH stretching and bending vibrations are detected at 2935 and 1382 cm^{-1}, respectively. The aromatic C═C stretching mode and the −CH bending mode in the $-CH_2$ group are located at 1462 and 1599 cm^{-1}, respectively.[40,41] On the other hand, α-CD shows absorption bands at 3397 cm^{-1}, which is for the O−H stretching frequency and nearly around 2926 cm^{-1} for the C−H stretching band, and two C−H bending vibrations appeared at 1414 and 1362 cm^{-1}, respectively.[42] The skeleton frequency, which is associated with the α-1, 4 linkage, is seen at 949 cm^{-1}, the C−O−C bending at 1154 cm^{-1}, and the C−C−O stretching at 1029 cm^{-1}. In the case of MEP + α-CD IC, the −OH bond stretching vibration has been noticed at 3424 cm^{-1}, whereas the −OH stretching frequency for the pure MEP was found at 3260 cm^{-1}, which suggests that the −OH group is inserted into the α-CD molecule's cavity. The aromatic C═C stretching and −CH stretching frequencies of the $-CH_3$ group appeared at 1599 and 2935 cm^{-1} in turn for the guest molecule and also moved to 1631 and 2924 cm^{-1}, respectively, in the MEP−α-CD inclusion complex. The −CH bending vibration also moved from 1454 to 1462 cm^{-1} after the inclusion complex formation. Thus, it may be inferred from the experimental results above that the alcoholic −OH group and the $-CH_3$ group of the aromatic moiety from the guest molecule MEP have been incorporated into the cavity of the α-CD host molecule.

Table 1. Experimental Information on the Chemical Shifts of Various Protons (in ppm) of [MEP], α-CD, and IC

guest	position of protons	pure guest chemical shift (ppm)	inclusion complex chemical shift (ppm) (IC)	change in chemical shift
MEP	H_f, H_g	6.905−6.853	6.885−6.833	**−0.020**
	H_d, H_e	7.155−7.127	7.128−7.109	**−0.027**
	H_c	4.001−3.972	4.024	0.023
	H_b	3.649−3.600	3.676−3.627	0.027
	H_a	3.911−3.901		
	$-CH_3$ protons	2.132	2.107	**−0.025**
α-CD	H-3	3.916−3.849	3.861−3.800	**−0.055**
	H-5	3.811−3.736	3.781−3.714	**−0.030**
	H-1	4.925−4.921	4.938	0.013
	H-2	3.513	3.529−3.503	0.016
	H-4	3.485−3.462	3.490−3.467	0.005

3.3. Job Plot Analysis. Using the UV−visible spectroscopic methodology, Job's technique offers a clear understanding of the stoichiometry of the IC synthesis in supramolecular host−guest chemistry.[34,43] To achieve this, different sets of MEP and α-CD solutions have been prepared with the variation of mole fraction varying between 0 and 1 for the drug molecule. We have plotted $\Delta A \times R$ against R to generate the graph, where R = [MEP]/([MEP] + [α-CD]) and ΔA represents the absorbance difference of MEP without and with α-CD. The absorbance data were precisely recorded for each solution at λ_{max} = 214 nm and 298.15 K (Table S1). It is possible to predict the stoichiometry of IC using the R values that show the largest variance, such as R = 0.5 for the host: guest ratio for a 1:1 complex, R = 0.33 for a 1:2 complex, and R = 0.66 for a 2:1 complex.[44−46] In the current study, maxima for the Job's plot were found at R = 0.5, signifying the creation of

https://doi.org/10.1021/acsomega.3c08185
ACS Omega 2024, 9, 36066−36075

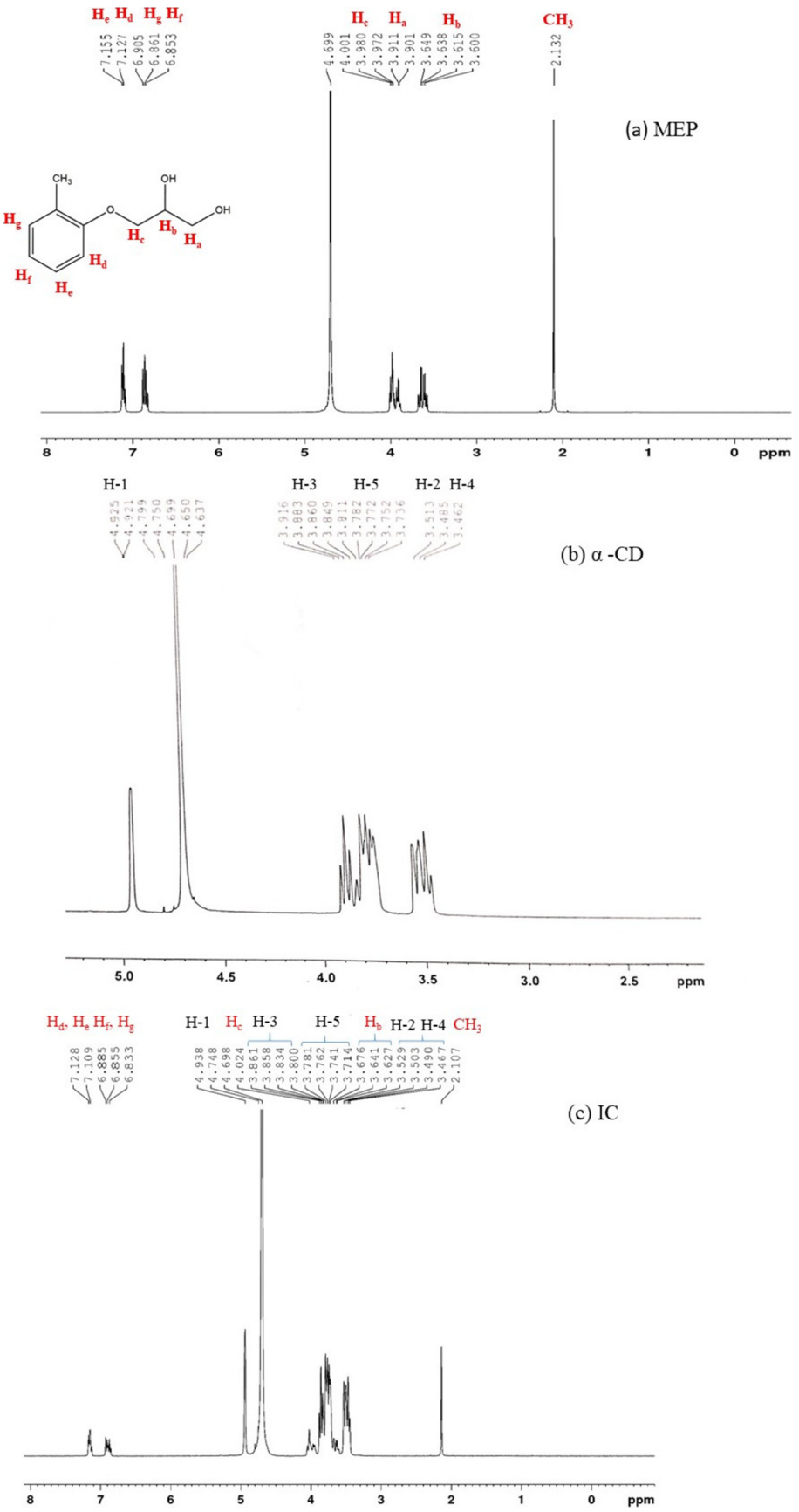

Figure 1. [1]H NMR of (a) [MEP], (b) α-CD, and (c) [MEP + α-CD] IC.

https://doi.org/10.1021/acsomega.3c08185
ACS Omega 2024, 9, 36066−36075

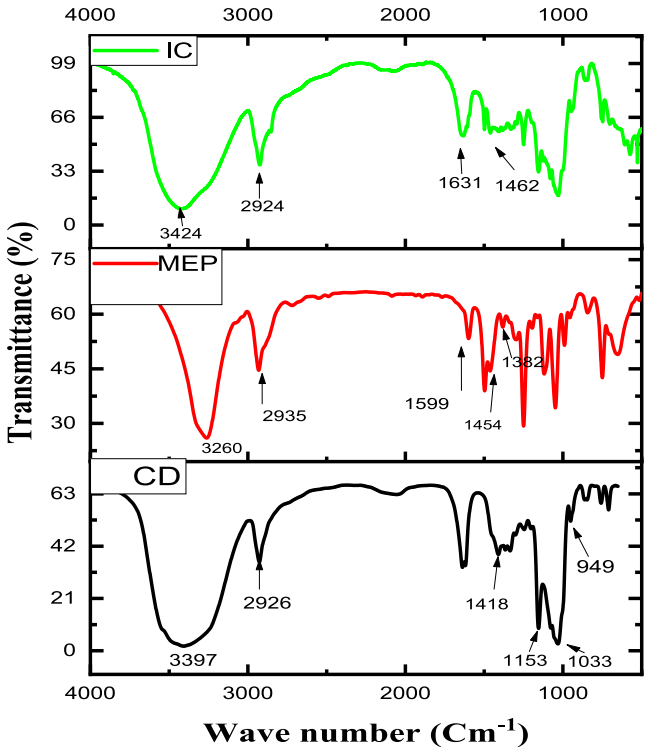

Figure 2. FT-IR spectra of α-CD, pure [MEP], and IC.

an inclusion complex with a 1:1 stoichiometry between MEP and α-CD (Figure 3).

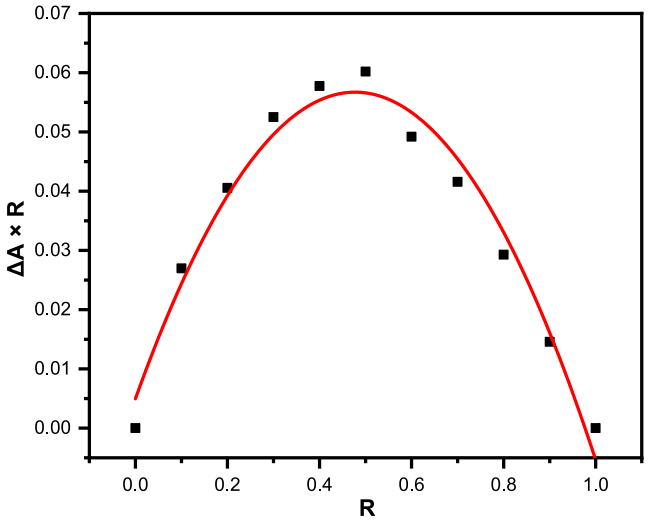

Figure 3. Job's plot for the [MEP] + α-CD system at 298.15 K at λ_{max} = 214 nm.

3.4. Association and Gibb's Free-Energy Determination. Association constants (K_a) have been used to analyze the stability of the complex and also the binding affinity of the IC produced among the pure MEP and α-CD using UV−vis spectroscopy.[34,47] The drug MEP is discovered to change its surroundings as it reaches the cavity of the α-CD molecule. The molar extinction coefficient (ε) is then altered as a result. A temperature change of 298.15 K was used to measure the variation in absorbance (ΔA) for MEP, whereas α-CD concentrations also varied (Table S2). One of the finest methods for determining the association constant (K_a) for 1:1 complexes is the Benesi−Hildebrand approach, which is illustrated below. Double reciprocal plots are created using the equation that follows (Figure 4)[48,49]

$$\frac{1}{\Delta A} = \frac{1}{\Delta\varepsilon[\mathrm{MEP}]K_a}\frac{1}{[\alpha\text{-CD}]} + \frac{1}{\Delta\varepsilon[\mathrm{MEP}]} \quad (1)$$

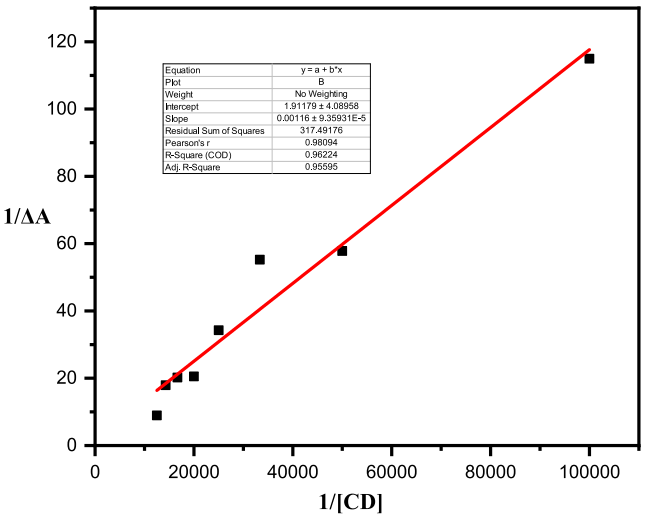

Figure 4. 1/absorbance vs 1/[α-CD] reciprocal plot.

where ΔA implies the difference in absorbance for the MEP with and without α-CD. The drug MEP's molar concentration is indicated by the symbol [MEP]. Equation 1 was used to determine the association constant (K_a) for (MEP + α-CD) IC based on the intercept/slope of the plots; the experimental value of K_a for IC was 1648.1 M^{-1} at 298.15 K (Figure 4).[50,51] The association constant (K_a) value was utilized to determine the free-energy change (ΔG), which came out to be −4.388 kcal/mol. From this, it can be inferred that the inclusion phenomenon is thermodynamically favorable when the ΔG is negative. This could be because of the occurrence of different kinds of connections, such as hydrogen bonding, hydrophobic interactions, and van der Waals interactions, between the MEP and α-CD during incorporation.

3.5. Powder XRD. Powder XRD is also a useful tool to investigate the development phenomenon of an inclusion complex formation from their parent molecules by relating the diffraction pattern of the parent samples and fashioning inclusion complex samples.[52,53] The diffraction patterns of α-CD, MEP, and IC are displayed in Figure 5. The characteristic peaks for α-CD are at 13.08, 15.11, 20.23, 21.15, 23.72, and 25.91 and for MEP at 13.62, 15.28, 16.38, 18.77, 21.53, and 22.99, respectively.[54] Because of the incorporation of the MEP into the α-CD molecule, some of their distinctive peaks vanished or become less intense in the MEP−αCD complex. The solid IC gives some major characteristic peaks at 5.93, 11.62, 12.16, 13.27, 15.46, and 19.69. From the above data, we have noticed that the IC formed from the parent molecules did not superimpose with the above characteristic peak, which implies that the formation of a new solid IC between MEP and α-CD is developed here.[55,56]

3.6. SEM Analysis. Another technique to find out the surface morphology of the solid sample is the scanning electron microscopy (SEM) analysis.[57] Here, we have seen that

https://doi.org/10.1021/acsomega.3c08185
ACS Omega 2024, 9, 36066−36075

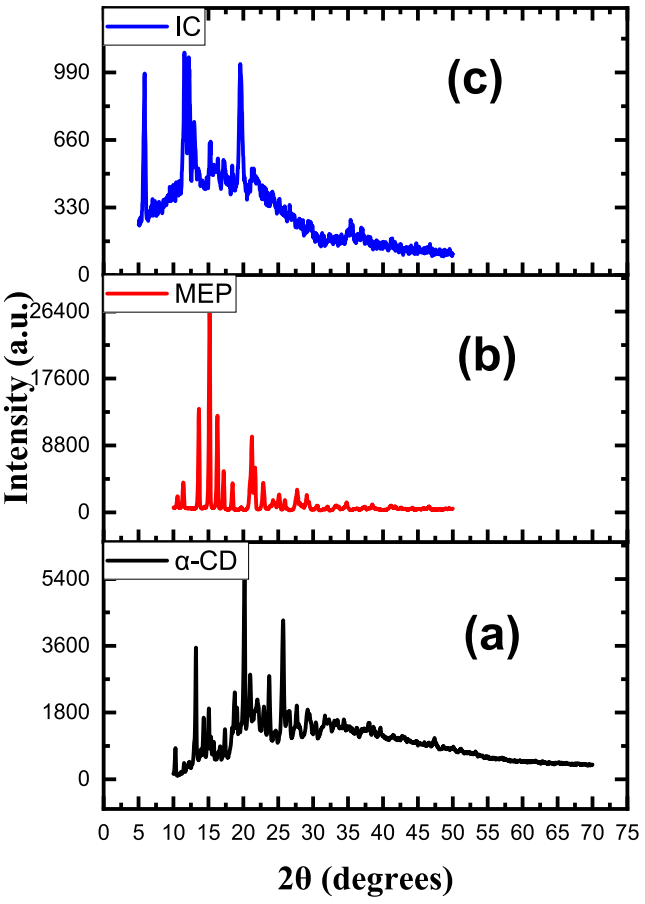

Figure 5. X-ray diffraction: (a) α-CD, (b) [MEP], and (c) IC.

the morphology of the solid IC formed from the host and guest molecules is completely different, which is shown in Figure 6. On SEM images, α-CD is detected as a cubic-type structure with large dimensions and MEP shows a long screw-type structure, whereas (MEP−αCD) IC is categorized as a needle-type structure, which is different from both the host and guest molecules. Hence, by comparing their morphology, it is clear that a solid IC is formed, and this morphology also supports the other analysis.[58]

3.7. TG Analysis. Thermogravimetric or TG analysis is another tool for measuring the thermal stability of pure drug MEP and its IC [MEP−αCD] formed from the host α-CD molecule.[59,60] The TGA curves for α-CD, pure MEP drug, and the [MEP−αCD] complex are shown in Figure 7. From the following three TGA curves it has been seen that pure MEP decomposes at the range of 190−260 °C, whereas the weight loss for α-CD has taken place through two stages, first, the weight loss is shown at around 98−105 °C, which may be due to the dehydration process and the second weight loss is noticed within the 280−340 °C range for the decomposition of α-CD. However, in the first stage, the [MEP−αCD] complex shows its weight loss at around 60−110 °C and the second stage at 250−350 °C finally continues up to 500 °C, indicating the development of the [MEP−αCD] complex. From the differential thermal analysis (DTA) curve, it has been seen that a characteristic endothermic peak of pure MEP, which was observed at 247 °C, completely vanished, and a new endothermic peak is observed in IC at 311 °C, which suggests that MEP had been completely incorporated into the cavity of α-CD.[61]

3.8. Molecular Docking Studies. To forecast how a guest would bind to the host cavity, molecular docking has been widely exploited.[62,63] PyRx software was used to perform the docking between MEP and α-CD. Figure 8 displays the optimal docked shape of the MEP−αCD complex (a, side view; b, top view). It was discovered that the MEP−α-CD complex's most stable docked conformation had the lowest negative binding energy (ΔG) value, which was −3.70 kcal/mol. This result closely resembles the value ($\simeq$−4.388 kcal/mol for MEP−α-CD) found in research using UV−visible spectroscopy, indicating a close correlation between the binding energy obtained from docking and the value obtained from UV−visible absorption analysis. The results of the docking process showed that in the MEP−α-CD complex's docked conformation, the benzene moiety of MEP was fully contained in the hydrophobic pocket of α-CD through to its wider edge, whereas the residual alkyl moiety of MEP was observed to exist outside the cavity's wider rim because of the smaller size of the cavity. Further, the docked conformation is seen to be stabilized by the electrostatic force between electronic clouds of benzene with the H-3 protons of α-CD. The docking study outcomes indicate that the interactions between MEP and α-CD are consistent with the findings of ^{1}H NMR and Fourier transform infrared spectroscopy (FT-IR) investigations.

3.9. Cytotoxicity Study. The chemicals α-CD, MEP, and MEP-IC were tested for their in vitro anticancer efficacy against the human renal adenocarcinoma cell line (ACHN). The IC_{50} value of α-CD (95.69 μg/mL) and MEP-IC (34.63

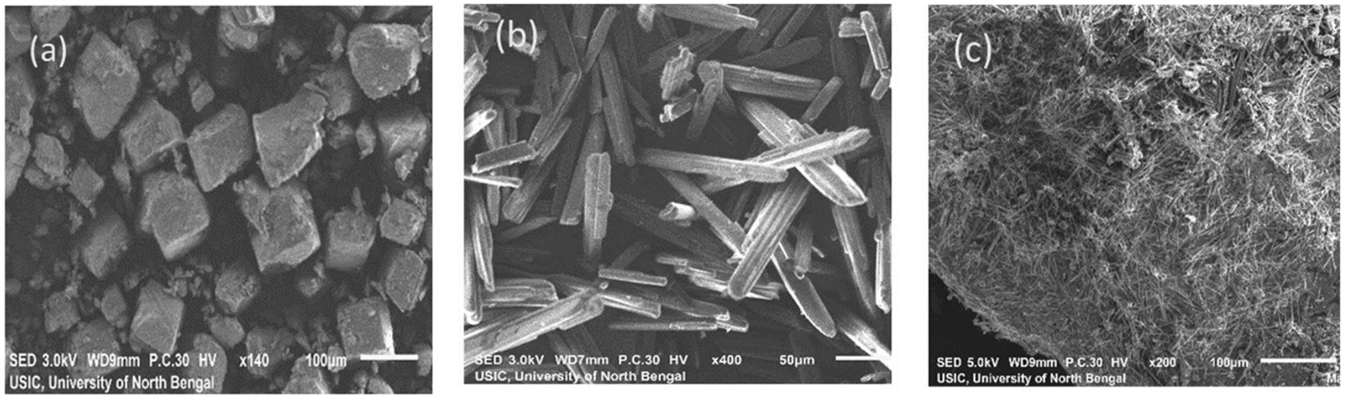

Figure 6. SEM images: (a) α-CD, (b) MEP, and (c) IC.

https://doi.org/10.1021/acsomega.3c08185
ACS Omega 2024, 9, 36066−36075

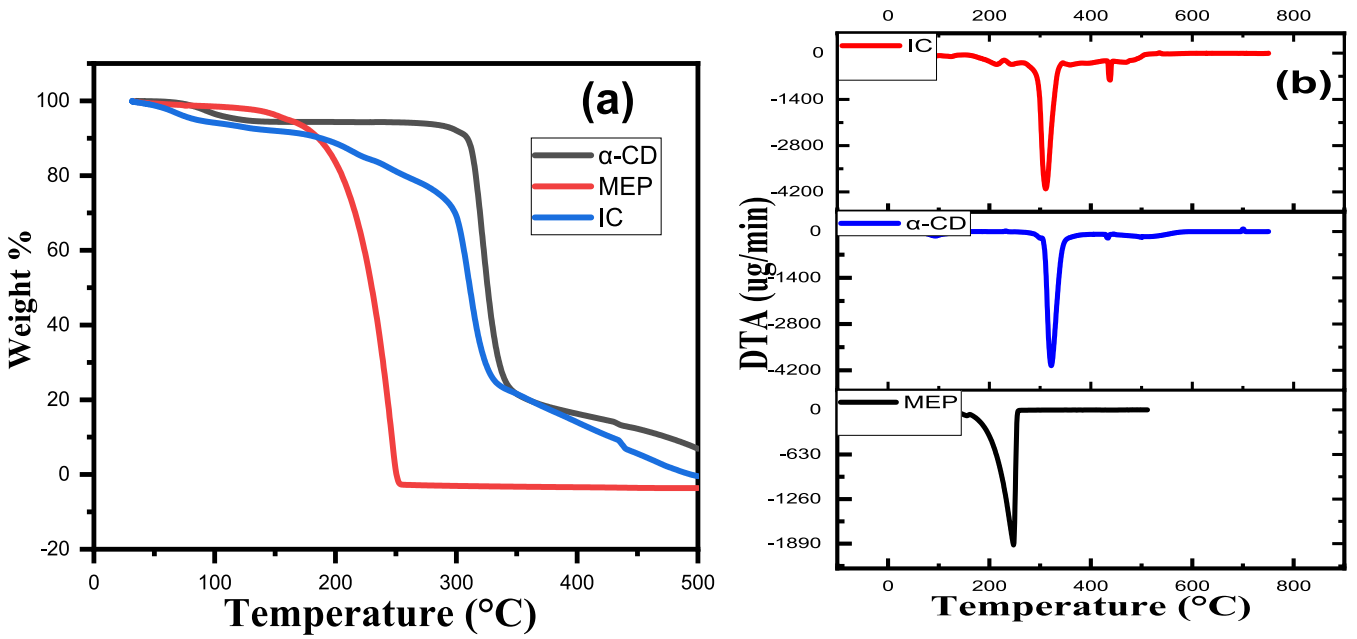

Figure 7. (a) TGA curve of IC, MEP, and α-CD; (b) DTA curve of MEP, α-CD, and IC.

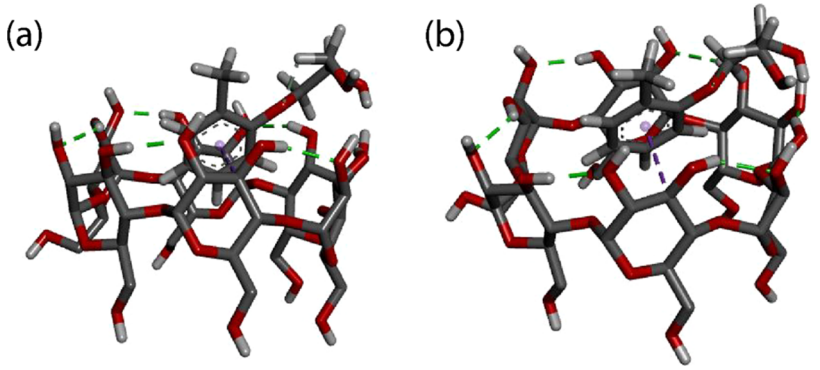

Figure 8. (a) Side view and (b) top view.

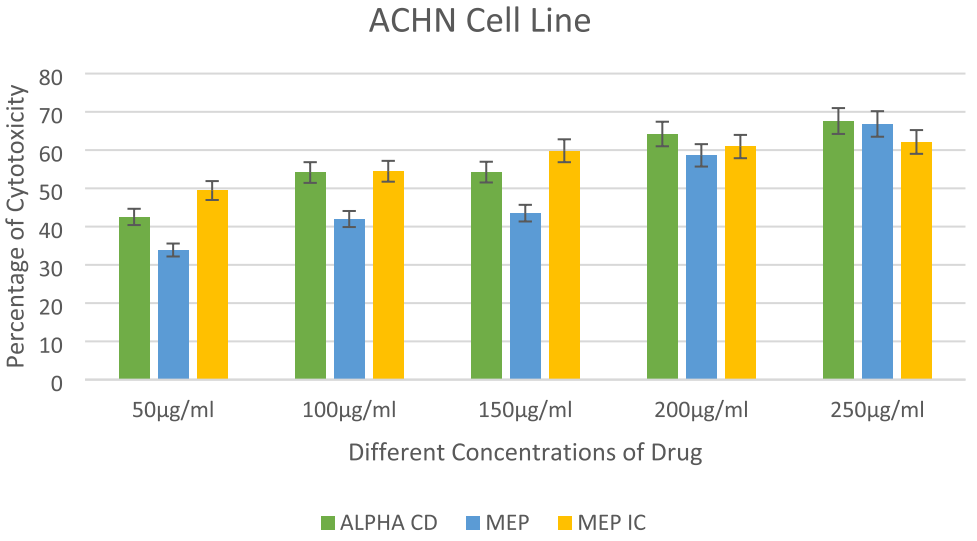

Figure 9. In vitro cell viability study of α-CD, MEP, and IC.

μg/mL) shows significant anticancer properties relative to MEP (156.24 μg/mL). Based on our results, we can conclude that the MEP-IC complex has anticancer activity against human renal adenocarcinoma and activity enhanced with the concentration of the complex. The MEP-IC complex shows better results in comparison to the other two complexes, α-CD

https://doi.org/10.1021/acsomega.3c08185
ACS Omega 2024, 9, 36066−36075

and MEP (Figures 9 and S1). So, we must say that MEP-IC would be a promising anticancer agent against human kidney cancer in the future.

3.10. Conclusions. Studies have been conducted on the inclusion phenomenon of α-CD with MEP medication. The results of the different characterization methods show that the method causes MEP to be encapsulated into the host α-CD's cavity, producing an innovative product called the MEP + α-CD complex, which has dissimilar properties and characteristics from both the host molecule (α-CD) and the guest molecule MEP. Through the use of ^{1}H NMR, IR, TGA, and UV−vis spectroscopy, the inclusion phenomena of MEP were revealed. Examining Job's graph reveals that ICs develop with a ratio of 1:1. The thermodynamic parameter ΔG^0 and stability constant K_a, which were determined using proven spectroscopic methods, support the thermodynamic feasibility of the inclusion and the stability of the newly formed IC, respectively. A thermodynamically favorable inclusion phenomenon is shown by the significant negative value of ΔG^0. The surface character of the inclusion complex was also ascertained with the aid of XRD and SEM analysis. The TGA measurement reveals that the IC exhibits greater thermal stability compared to that of the guest molecule. The molecular docking analysis provides information on the virtually identical orientations of the MEP drug's binding mode into the α-CD cavity, which are supported by the results of ^{1}H NMR as well as FT-IR. The cytotoxicity study of [MEP] and IC compounds against human renal adenocarcinoma cell line (ACHN) observed that the MEP-IC complex shows better results in comparison to the other two compounds like α-CD and MEP and hence it would be a promising anticancer agent against human kidney cancer in future.

■ ASSOCIATED CONTENT

Supporting Information

The Supporting Information is available free of charge at https://pubs.acs.org/doi/10.1021/acsomega.3c08185.

Job's plot data, table for association constant, and graph of cell viability study (PDF)

■ AUTHOR INFORMATION

Corresponding Author

Mahendra Nath Roy − *Department of Chemistry, University of North Bengal, Darjeeling, West Bengal 734013, India;* orcid.org/0000-0002-7380-5526; Email: mahendraroy2002@yahoo.co.in, mahendraroy2018@nbu.ac.in

Authors

Subhajit Debnath − *Department of Chemistry, University of North Bengal, Darjeeling, West Bengal 734013, India*

Biswajit Ghosh − *Department of Chemistry, University of North Bengal, Darjeeling, West Bengal 734013, India*

Modhusudan Mondal − *Department of Chemistry, University of North Bengal, Darjeeling, West Bengal 734013, India*

Niloy Roy − *Department of Chemistry, University of North Bengal, Darjeeling, West Bengal 734013, India*

Kangkan Mallick − *Department of Chemistry, University of North Bengal, Darjeeling, West Bengal 734013, India*

Joydeb Maji − *Department of Botany, Siliguri College, Darjeeling, West Bengal 734001, India*

Sudip Sahana − *Department of Chemistry, Saldiha College, Bankura, West Bengal 722136, India*

Anuradha Sinha − *Department of Chemistry, Siliguri College, Darjeeling, West Bengal 734001, India*

Sangita Dey − *Department of Biotechnology, University of North Bengal, Darjeeling, West Bengal 734013, India*

Anoop Kumar − *Department of Biotechnology, University of North Bengal, Darjeeling, West Bengal 734013, India*

Complete contact information is available at: https://pubs.acs.org/10.1021/acsomega.3c08185

Author Contributions

M.N.R. and S.D.: conceptualization and resources. M.N.R.: supervision and cosupervision. A.S., S.D., and M.M.: writing—review and editing. S.D., B.G., and N.R.: investigation, writing—original draft, methodology, software, and formal analysis. S.D., S.S., J.M., K.M., A.S., M.N.R., S.D., and A.K.: validation, investigation, and visualization.

Notes

The authors declare no competing financial interest.

■ ACKNOWLEDGMENTS

The authors express their gratitude to DST-SAIF Cochin for providing the sample's FT-IR, TGA, and PXRD analyses, as well as for the cooperation of the University of North Bengal's Department of Chemistry.

■ ABBREVIATIONS

MEP: mephenesin
α-CD: α-cyclodextrin
IC: inclusion complex
FT-IR: Fourier transform infrared spectroscopy
NMR: nuclear magnetic resonance
TGA: thermogravimetric analysis
SEM: scanning electron microscopy
PXRD: powder X-ray diffraction
MEP-IC: mephenesin-inclusion complex

■ REFERENCES

(1) Gonzalez-Garay, A.; Gonzalez-Miquel, M.; Guillen-Gosalbez, G. High-value propylene glycol from low-value biodiesel glycerol: a techno-economic and environmental assessment under uncertainty. *ACS Sustainable Chem. Eng.* **2017**, *5* (7), 5723−5732.

(2) Dye, R. F. Ethylene glycols technology. *Korean J. Chem. Eng.* **2001**, *18*, 571−579.

(3) Ludwig, B. J.; West, W. A.; Currie, W. E. Muscle-paralyzing compounds related to mephenesin. *J. Am. Chem. Soc.* **1952**, *74* (8), 1935−1939.

(4) Wermuth, C. G.; Lesuisse, D. Preparation of Water-Soluble Compounds by Covalent Attachment of Solubilizing Moieties. *Med. Chem.* **2015**, *30*, 723−745.

(5) Bock, M. G.; DiPardo, R. M.; Mellin, E. C.; Newton, R. C.; Veber, D. F.; Freedman, S. B.; Freidinger, R. M.; et al. Second-generation benzodiazepine CCK-B antagonists. Development of subnanomolar analogs with selectivity and water solubility. *J. Med. Chem.* **1994**, *37* (6), 722−724.

(6) Shen, S.; Shi, H.; Sun, H. Kinetics and mechanism of oxidation of the drug mephenesin by bis (hydrogenperiodato) argentate (III) complex anion. *Int. J. Chem. Kinet.* **2007**, *39* (8), 440−446.

(7) Galletti, G.; Prete, P.; Vanzini, S.; Cucciniello, R.; Fasolini, A.; Maron, J. De.; Cavani, F.; Tabanelli, T. Glycerol Carbonate as a Versatile Alkylating Agent for the Synthesis of β-Aryloxy Alcohols. *ACS Sustainable Chem. Eng.* **2022**, *10*, 10922−10933.

(8) Crankshaw, D. P.; Raper, C. Mephenesin, methocarbamol, chlordiazepoxide and diazepam: actions on spinal reflexes and ventral root potentials. *Br. J. Pharmacol.* **1970**, *38*, 1476−5381.
(9) Thomas, N. S.; George, K.; Selvam, A. A. A. Troxerutin subdues hepatic tumorigenesis via disrupting the MDM2-p53 interaction. *Food Funct.* **2018**, *9* (10), 5336−5349.
(10) Theil, F.; Ballschuh, S.; Kunath, A.; Schick, H. Kinetic resolution of rac-3-(2-methylphenoxy)propane-1,2-diol (mephenesin) by sequential lipase-catalyzed transesterification. *Tetrahedron: Asymmetry* **1991**, *2*, 1031−1034.
(11) Crankshaw, D. P.; Raper, C. Some studies on peripheral actions of mephenesin, methocarbamol and diazepam. *Br. J. Pharmacol.* **1968**, *34*, 579.
(12) Godman, H. E. Mephenesin as a relaxing agent in the treatment of tetanus—clinical experience in 12 cases. *Calif. Med.* **1951**, *74* (2), 126−127.
(13) Del Valle, E. M. Cyclodextrins and their uses: a review. *Process Biochem.* **2004**, *39* (9), 1033−1046.
(14) Strokopytov, B.; Penninga, D.; Rozeboom, H. J.; Kalk, K. H.; Dijkhuizen, L.; Dijkstra, B. W. X-ray structure of cyclodextrin glycosyltransferase complexed with acarbose. Implications for the catalytic mechanism of glycosidases. *Biochemistry* **1995**, *34* (7), 2234−2240.
(15) Cai, L.; Jeremic, D.; Lim, H.; Kim, Y. β-Cyclodextrins as sustained-release carriers for natural wood preservatives. *Ind. Crops Prod.* **2019**, *130*, 42−48.
(16) Li, H.; Chen, D. X.; Sun, Y. L.; Zheng, Y. B.; Tan, L. L.; Weiss, P. S.; Yang, Y. W. Viologen-mediated assembly of and sensing with carboxylatopillar [5] arene-modified gold nanoparticles. *J. Am. Chem. Soc.* **2013**, *135* (4), 1570−1576.
(17) Negi, J. S.; Singh, S. Spectroscopic investigation on the inclusion complex formation between amisulpride and γ-cyclodextrin. *Carbohydr. Polym.* **2013**, *92* (2), 1835−1843.
(18) Ghosh, B.; Roy, N.; Roy, D.; Mandal, S.; Mondal, M.; Dakua, V. K.; Roy, M. N.; et al. Exploring Inclusion Complex of an Antithyroid Drug (PTU) with α-Cyclodextrin for Innovative Applications by Physicochemical Approach Optimized by Molecular Docking. *J. Mol. Liq.* **2023**, *380*, No. 121708.
(19) Ceborska, M. Interactions of native cyclodextrins with biorelevant molecules in the solid state: A review. *Curr. Org. Chem.* **2014**, *18* (14), 1878−1885.
(20) Bomzan, P.; Roy, N.; Sharma, A.; Rai, V.; Ghosh, S.; Kumar, A.; Roy, M. N. Molecular encapsulation study of indole-3-methanol in cyclodextrins: Effect on antimicrobial activity and cytotoxicity. *J. Mol. Struct.* **2021**, *1225*, No. 129093.
(21) Ghosh, R.; Roy, K.; Subba, A.; Mandal, P.; Basak, S.; Kundu, M.; Roy, M. N. Case to case study for exploring inclusion complexes of an anti-diabetic alkaloid with α and β cyclodextrin molecules for sustained dischargement. *J. Mol. Struct.* **2020**, *1200*, No. 126988.
(22) Tian, B.; Hua, S.; Liu, J. Cyclodextrin-based delivery systems for chemotherapeutic anticancer drugs: A review. *Carbohydr. Polym.* **2020**, *232*, No. 115805.
(23) Puliti, R.; Mattia, C. A.; Paduano, L. Crystal structure of a new α-cyclodextrin hydrate form. Molecular geometry and packing features: disordered solvent contribution. *Carbohydr. Res.* **1998**, *310* (1−2), 1−8.
(24) Sompornpisut, P.; Deechalao, N.; Vongsvivut, J. (2002). An inclusion complex of β-Cyclodextrin-L-Phenylalanine: 1H NMR and molecular docking studies. *Sci. Asia* **2002**, *28*, 263−270.
(25) Roy, N.; Bomzan, P.; Ghosh, B.; Roy, M. N. A combined experimental and theoretical study on p-sulfonatothiacalix [4] arene encapsulated sulisobenzone. *New J. Chem.* **2023**, *47* (3), 1045−1049.
(26) Dallakyan, S.; Olson, A. J. Small-Molecule Library Screening by Docking with PyRx. In *Chemical Biology: Methods and Protocols*; Springer, 2015; Vol. *1263*, pp 243−250.
(27) Kanchana, S.; Kaviya, T.; Rajkumar, P.; Kumar, M. D.; Elangovan, N.; Sowrirajan, S. Computational investigation of solvent interaction (TD-DFT, MEP, HOMO-LUMO), wavefunction studies and molecular docking studies of 3-(1-(3-(5-((1-methylpiperidin-4-yl) methoxy) pyrimidin-2-yl) benzyl)-6-oxo-1, 6-dihydropyridazin-3-yl) benzonitrile. *Chem. Phys. Impact* **2023**, *7*, No. 100263.
(28) Mondal, M.; Basak, S.; Roy, D.; Haydar, M. S.; Choudhury, S.; Ghosh, B.; Roy, M. N.; et al. Probing the molecular assembly of a metabolizer drug with β-cyclodextrin and its binding with CT-DNA in augmenting antibacterial activity and photostability by physicochemical and computational methodologies. *ACS Omega* **2022**, *7* (30), 26211−26225.
(29) Mondal, M.; Basak, S.; Roy, D.; Saha, S.; Ghosh, B.; Ali, S.; Roy, M. N.; et al. Cyclic oligosaccharides as controlled release complexes with food additives (TZ) for reducing hazardous effects. *J. Mol. Liq.* **2022**, *348*, No. 118429.
(30) Srinivasan, K.; Sivakumar, K.; Stalin, T. 2, 6-Dinitroaniline and β-cyclodextrin inclusion complex properties studied by different analytical methods. *Carbohydr. Polym.* **2014**, *113*, 577−587.
(31) Bani-Yaseen, A. D.; Mo'ala, A. (2014). Spectral, thermal, and molecular modeling studies on the encapsulation of selected sulfonamide drugs in β-cyclodextrin nano-cavity. *Spectrochim. Acta, Part A* **2014**, *131*, 424−431.
(32) Wang, L.; Li, S.; Tang, P.; Yan, J.; Xu, K.; Li, H. Characterization and evaluation of synthetic riluzole with β-cyclodextrin and 2, 6-di-O-methyl-β-cyclodextrin inclusion complexes. *Carbohydr. Polym.* **2015**, *129*, 9−16.
(33) Saha, S.; Ray, T.; Basak, S.; Roy, M. N. NMR, surface tension and conductivity studies to determine the inclusion mechanism: thermodynamics of host−guest inclusion complexes of natural amino acids in aqueous cyclodextrins. *New. J. Chem.* **2016**, *40* (1), 651−661.
(34) Caso, J. V.; Russo, L.; Palmieri, M.; Malgieri, G.; Galdiero, S.; Falanga, A.; Isernia, C.; Iacovino, R. Investigating the inclusion properties of aromatic amino acids complexing beta-cyclodextrins in model peptides. *Amino Acids* **2015**, *47*, 2215−2227.
(35) Wang, T.; Wang, M.; Ding, C.; Fu, J. Mono-benzimidazole functionalized β-cyclodextrins as supramolecular nanovalves for pH-triggered release of p-coumaric acid. *Chem. Commun.* **2014**, *50* (83), 12469−12472.
(36) Roy, A.; Saha, S.; Roy, D.; Bhattacharyya, S.; Roy, M. N. Formation & specification of host−guest inclusion complexes of an anti-malarial drug inside into cyclic oligosaccharides for enhancing bioavailability. *J. Inclusion Phenom. Macrocyclic Chem.* **2020**, *97*, 65−76.
(37) Sierpe, R.; Noyong, M.; Simon, U.; Aguayo, D.; Huerta, J.; Kogan, M. J.; Yutronic, N. Construction of 6-thioguanine and 6-mercaptopurine carriers based on βcyclodextrins and gold nanoparticles. *Carbohydr. Polym.* **2017**, *177*, 22−31.
(38) Benesi, H. A.; Hildebrand, J. H. J. A spectrophotometric investigation of the interaction of iodine with aromatic hydrocarbons. *J. Am. Chem. Soc.* **1949**, *71* (8), 2703−2707.
(39) Doan, L. A.; Ghatten, L. G. Identification and Differentiation of Organic Medicinal Agents II: Muscle Relaxants. *J. Pharm. Sci.* **1965**, *54* (11), 1605−1609.
(40) Wadhwani, M.; Jain, S. Ultraviolet light induced oxidation of malonic acid by chloramine-T in an aqueous acidic medium: A kinetic study. *Ind. J. Adv. Chem. Sci.* **2016**, *40* (1), 36−39.
(41) Kumar, A.; Sharma, G.; Naushad, M.; Thakur, S. SPION/β-cyclodextrin core−shell nanostructures for oil spill remediation and organic pollutant removal from waste water. *Chem. Eng. J.* **2015**, *280*, 175−187.
(42) Li, W.; Lu, B.; Sheng, A.; Yang, F.; Wang, Z. Spectroscopic and theoretical study on inclusion complexation of beta-cyclodextrin with permethrin. *J. Mol. Struct.* **2010**, *981* (1−3), 194−203.
(43) Roy, M. N.; Roy, A.; Saha, S. Probing inclusion complexes of cyclodextrins with amino acids by physicochemical approach. *Carbohydr. Polym.* **2016**, *151*, 458−466.
(44) Saha, S.; Roy, A.; Roy, K.; Roy, M. N. Study to explore the mechanism to form inclusion complexes of β-cyclodextrin with vitamin molecules. *Sci. Rep.* **2016**, *6* (1), No. 35764.
(45) Dotsikas, Y.; Kontopanou, E.; Allagiannis, C.; Loukas, Y. L. Interaction of 6-p-toluidinylnaphthalene-2-sulphonate with β-cyclodextrin. *J. Pharm. Biomed. Anal.* **2000**, *23* (6), 997−1003.

https://doi.org/10.1021/acsomega.3c08185
ACS Omega 2024, 9, 36066−36075

(46) Cramer, F.; Saenger, W.; Spatz, H. C. Inclusion compounds. XIX. 1a The formation of inclusion compounds of α-cyclodextrin in aqueous solutions. Thermodynamics and kinetics. *J. Am. Chem. Soc.* **1967**, *89* (1), 14−20.
(47) Maass, A. R.; Carey, P. L.; Heming, A. E. Spectrophotometric Determination of 3-o-Tolyloxy-1, 2-propanediol (Mephenesin) and Its Metabolite in Plasma and Urine. *Anal. Chem.* **1959**, *31* (8), 1331−1334.
(48) Ge, X.; Huang, Z.; Tian, S.; Huang, Y.; Zeng, C. Complexation of carbendazim with hydroxypropyl-β-cyclodextrin to improve solubility and fungicidal activity. *Carbohydr. Polym.* **2012**, *89* (1), 208−212.
(49) Roy, N.; Bomzan, P.; Roy, D.; Ghosh, B.; Roy, M. N. Exploring β-CD grafted GO nanocomposites with an encapsulated fluorescent dye duly optimized by molecular docking for better applications. *J. Mol. Liq.* **2021**, *329*, No. 115481.
(50) Roy, N.; Bomzan, P.; Roy, M. N. Probing Host-Guest inclusion complexes of Ambroxol Hydrochloride with α-& β-Cyclodextrins by physicochemical contrivance subsequently optimized by molecular modeling simulations. *Chem. Phys. Lett.* **2020**, *748*, No. 137372.
(51) Roy, N.; Ghosh, B.; Roy, D.; Bhaumik, B.; Roy, M. N. Exploring the inclusion complex of a drug (umbelliferone) with α-cyclodextrin optimized by molecular docking and increasing bioavailability with minimizing the doses in human body. *ACS Omega* **2020**, *5* (46), 30243−30251.
(52) Chen, M.; Diao, G.; Zhang, E. Study of inclusion complex of β-cyclodextrin and nitrobenzene. *Chemosphere* **2006**, *63* (3), 522−529.
(53) Bera, H.; Chekuri, S.; Sarkar, S.; Kumar, S.; Muvva, N. B.; Mothe, S.; Nadimpalli, J. Novel pimozide-β-cyclodextrin-polyvinyl-pyrrolidone inclusion complexes for Tourette syndrome treatment. *J. Mol. Liq.* **2016**, *215*, 135−143.
(54) Jiao, H.; Goh, S. H.; Valiyaveettil, S.; Zheng, J. Inclusion complexes of perfluorinated oligomers with cyclodextrins. *Macromolecules* **2003**, *36* (11), 4241−4243.
(55) Grebogi, I. H.; Tibola, A. P. O.; Barison, A.; Grandizoli, C. W.; Ferraz, H. G.; Rodrigues, L. N. Binary and ternary inclusion complexes of dapsone in cyclodextrins and polymers: preparation, characterization and evaluation. *J. Inclusion Phenom. Macrocyclic Chem.* **2012**, *73*, 467−474.
(56) Van den Mooter, G.; Augustijns, P.; Blaton, N.; Kinget, R. Physico-chemical characterization of solid dispersions of temazepam with polyethylene glycol 6000 and PVP K30. *Int. J. Pharm.* **1998**, *164* (1−2), 67−80.
(57) Wang, J.; Cao, Y.; Sun, B.; Wang, C. Characterisation of inclusion complex of trans-ferulic acid and hydroxypropyl-β-cyclodextrin. *Food Chem.* **2011**, *124* (3), 1069−1075.
(58) Ghosh, R.; Ekka, D.; Rajbanshi, B.; Yasmin, A.; Roy, M. N. Synthesis, characterization of 1-butyl-4-methylpyridinium lauryl sulfate and its inclusion phenomenon with β-cyclodextrin for enhanced applications. *Colloids, Surf. A* **2018**, *548*, 206−217.
(59) Chakraborty, S.; Ghosh, P.; Basu, B.; Mandal, A. Inclusion complex of β-cyclodextrin with tetrabutylammonium bromide: Synthesis, characterization and interaction with calf thymus DNA. *J. Mol. Liq.* **2019**, *293*, No. 111525.
(60) Kayaci, F.; Uyar, T. Solid inclusion complexes of vanillin with cyclodextrins: their formation, characterization, and high-temperature stability. *J. Agric. Food Chem.* **2011**, *59* (21), 11772−11778.
(61) Ai, L.; Hu, J.; Ji, X.; Zhao, H. Structure confirmation and thermal kinetics of the inclusion of cis-jasmone in β-cyclodextrin. *RSC Adv.* **2019**, *9*, 26224−26229.
(62) Rezende, A. A.; Santos, R. S.; Andrade, L. N.; Amaral, R. G.; Pereira, M. M.; Bani, C.; Severino, P.; et al. Anti-tumor efficiency of perillylalcohol/β-cyclodextrin inclusion complexes in a sarcoma S180-induced mice model. *Pharmaceutics* **2021**, *13* (2), 245.
(63) Mady, F. M.; Farghaly Aly, U. Experimental, molecular docking investigations and bioavailability study on the inclusion complexes of finasteride and cyclodextrins. *Drug Des., Dev. Ther.* **2017**, *11*, 1681−1692.

https://doi.org/10.1021/acsomega.3c08185
ACS Omega 2024, 9, 36066−36075